Atmos. Chem. Phys. Discuss., 15, 7977–8015, 2015
www.atmos-chem-phys-discuss.net/15/7977/2015/
doi:10.5194/acpd-15-7977-2015

Atmospheric Chemistry and Physics Discussions

VOC species and emission inventory from vehicles and their SOA formation potentials estimation in Shanghai, China

C. Huang[1], H. L. Wang[1], L. Li[1], Q. Wang[1], Q. Lu[1], J. A. de Gouw[2], M. Zhou[1], S. A. Jing[1], J. Lu[1], and C. H. Chen[1]

[1]State Environmental Protection Key Laboratory of the Formation and Prevention of Urban Air Pollution Complex, Shanghai Academy of Environmental Sciences, Shanghai, China
[2]Earth System Research Laboratory, Chemical Sciences Division, NOAA, 325 Broadway, Boulder, Colorado 80305, USA

Received: 22 December 2014 – Accepted: 17 February 2015 – Published: 17 March 2015

Correspondence to: C. Huang (huangc@saes.sh.cn)

Published by Copernicus Publications on behalf of the European Geosciences Union.

Abstract

VOC species from vehicle exhaust and gas evaporation were investigated by chassis dynamometer and on-road measurements of 9 gasoline vehicles, 7 diesel vehicles, 5 motorcycles, and 4 gas evaporation samples. The SOA mass yields of gasoline, diesel, motorcycle exhausts, and gas evaporation were calculated based on the mixing ratio of individual VOC species. The SOA mass yields of gasoline and motorcycle exhaust were similar to the results of the published smog chamber study with the exception of that of diesel exhaust was 20 % lower than experimental data (Gordon et al., 2013, 2014a, b). This suggests the requirement for further research on SVOC or LVOC emissions. A vehicular emission inventory was compiled based on a local survey of vehicle mileage traveled and real-world measurements of vehicle emission factors. The inventory-based vehicular initial emission ratio of OA to CO was 15.6 $\mu g\,m^{-3}\,ppmv^{-1}$. The OA production rate reached 22.3 and 42.7 $\mu g\,m^{-3}\,ppmv^{-1}$ under high-NO_x and low-NO_x conditions, respectively. To determine the vehicular contribution to OA pollution, the inventory-based OA formation ratios for vehicles were calculated with a photochemical-age-based parameterization method and compared with the observation-based OA formation ratios in the urban atmosphere of Shanghai. The results indicated that VOC emissions from vehicle exhaust and gas evaporation only explained 15 and 22 % of the total organic aerosols observed in summer and winter, respectively. SOA production only accounted for 25 and 18 % of the total vehicular OA formation in summer and winter. VOC emissions from gasoline vehicles contribute 21–38 % of vehicular OA formation after 6–24 h of photochemical aging. The results suggest that vehicle emissions are an important contributor to OA pollution in the urban atmosphere of Shanghai. However, a large number of OA mass in the atmosphere still cannot be explained in this study. SOA formation contributions from other sources (e.g. coal burning, biomass burning, cooking, dust, etc.) as well as IVOCs and SVOCs from the combustion sources need to be considered in future studies.

ACPD
15, 7977–8015, 2015

1 Introduction

Secondary organic aerosol (SOA) accounts for a significant fraction of ambient tropospheric aerosol (Hallquist et al., 2009; Jimenez et al., 2009). De Gouw and Jimenez (2009) suggested that SOA from urban sources may be the dominant source of organic aerosol globally between 30 and 50° latitude.

Gas-phase oxidation of volatile organic compounds (VOCs) has traditionally been considered to be the major source of urban SOA formation. VOCs are oxidized to low vapor pressure reaction products by OH radical, ozone, and NO_3 radical, and eventually form organic aerosol (OA) in the atmosphere. Odum et al. (1997) investigated the SOA formation from vaporized reformulated gasoline and found single light aromatic hydrocarbons are responsible for the majority of SOA formation. Kleindienst et al. (2002) verified that 75–85 % of the SOA was due to reaction products of C6–C9 light aromatic compounds from automobile exhaust. Robinson et al. (2007) further recognized that intermediate-volatility organic compounds (IVOCs) and semi-volatility organic compounds (SVOCs) are also important sources for OA production based on the smog chamber studies of diesel exhaust and wood fire (Weitkamp et al., 2007; Grieshop et al., 2009). Their subsequent study pointed IVOCs such as long-chain and branched alkanes from vehicle exhaust play more important roles in SOA production compared with other combustion emissions (Jathar et al., 2013). A recent study from Zhao et al. (2014) concluded that primary IVOCs were estimated to produce about 30 % of newly formed SOA in the afternoon during CalNex campaign in Pasadena, California.

Due to the abundance of reactive organic compounds, vehicle emission has been recognized as a major source of urban SOA formation (Stone et al., 2009; Liu et al., 2012; Borbon et al., 2013). Laboratory chamber studies also report significant SOA production from diesel, gasoline, and motorcycle exhaust photo-oxidation (Hung et al., 2006; Weitkamp et al., 2007; Chirico et al., 2010; Nordin et al., 2013; Platt et al., 2013). Current research is now focusing on the relative importance of gasoline and diesel ve-

ACPD
15, 7977–8015, 2015

hicles to urban SOA formation. Bahreini et al. (2012) and Hayes et al. (2013) suggested gasoline emissions dominate over diesel in urban SOA formation by field studies. Gentner et al. (2012) argued diesel is responsible for 65 to 90 % of vehicular-derived SOA based on the estimation of SOA formation from gasoline and diesel fuel compositions. Considering the importance of vehicular gas-phase precursors to SOA formation prediction, May et al. (2014) investigated the VOC emissions from 64 light-duty gasoline vehicles, 2 medium-duty diesel vehicles and 3 heavy-duty diesel vehicles with varying levels of aftertreatment.

Shanghai is one of the most urbanized cities in the Yangtze River Delta (YRD) region in China. The YRD region occupies 2 % of land area and generates 8–12 % of the primary $PM_{2.5}$ and the emissions of its precursors in China (Huang et al., 2011). Motor vehicles are the fastest growing source of pollution in the megacities of China. The number of vehicles in Shanghai increased to 1.9 times of the number in the last decade and reached 2.6 million (about 107 units per 1000 capita) in 2012 (SCCTPI, 2013). Gasoline and diesel vehicles increased by 2.8 and 1.3 times, respectively, while motorcycle decreased by 36 %. Vehicular emission has been recognized as the largest source of VOCs in urban Shanghai, which contributes 25 ~ 28 % of the measured VOC concentrations. Other VOC emission sources were solvent usage, chemical industry, petrochemical industry, and coal burning, etc. (Cai et al., 2010; Wang et al., 2013). Yuan et al. (2013) indicated that VOC emissions are large contributors to SOA formation through field measurements at a receptor site in eastern China. Huang et al. (2012, 2013) reported that 28.7–32.1 % of the fine particle mass is organic matter (OM) and 30.2–76 % of OM is contributed by SOA in the atmosphere of Shanghai and its surrounding areas. Based on the historical measurement data of organic (OC) and element carbon (EC) in $PM_{2.5}$ in the atmosphere in urban Shanghai, the OC/EC ratio shows growing trend from 1999 to 2011, which implies that the secondary fraction of organic matter is playing an increasing role in urban Shanghai (Ye et al., 2003; Feng et al., 2005, 2013; Hou et al., 2011; Cao et al., 2013).

ACPD
15, 7977–8015, 2015

However, the contribution of VOC emissions to SOA formation and the relative importance of vehicular emission remain unclear. At present, vehicle use is experiencing a rapid growth episode in the cities of China. Understanding the contribution of vehicular VOC emissions to SOA formation will be helpful to identify the source of OA and $PM_{2.5}$ pollution in China. In this study, we first investigated the VOC species from gasoline, diesel, and motorcycle exhausts and gas evaporation. Then, we compiled a vehicular emission inventory for Shanghai and estimated the SOA formation potential from vehicles based on the SOA mass yields of different vehicle types by a photochemical-age-based parameterization method. Vehicular contributions to OA pollution were compared with the inventory-based vehicular OA production using the observed OA formation ratios in summer and winter in the urban atmosphere of Shanghai.

2 Materials and methods

2.1 Vehicular VOC species sampling and analysis

The exhaust from 4 light-duty gasoline vehicles (LDGVs), 5 taxis, 5 heavy-duty diesel trucks (HDDTs), 2 city buses (buses), and 5 motorcycles (MTs) were measured in June 2010. LDGVs, taxis, and MTs were fueled by gasoline. HDDTs and buses were fueled by diesel. The emission standards of the tested vehicles covered Euro 1 to Euro 3 and their model years covered 2001 to 2009. All MTs were 4-stroke with 125 cc displacement. Table 1 lists the detailed information of the tested vehicles. Commercially available fuels were used in the test. The fuel quality met the requirements of the local standard in Shanghai. The sulfur contents of both gasoline and diesel fuel were below 50 ppm.

All the automobiles were measured on chassis dynamometers. LDGVs and taxis were measured utilizing a vehicle mass analysis system (VMAS), which was widely used in in-use vehicle inspection stations in China. The driving cycle of VMAS con-

ACPD
15, 7977–8015, 2015

tains only 1 bag from ECE urban cycle. The highest speed reaches 50 km h^{-1} and the average speed is about 18.8 km h^{-1}. HDDTs and buses were measured on a loaded mode test cycle. The tested vehicles were operated on idling and a test cycle which simulates high engine loads under 100, 90, and 80 % of their maximum powers. The highest speed reaches 70 km h^{-1}. MT exhausts were sampled while operating on the road. A GPS unit was installed on the tested motorcycles to record the speeds second by second. The highest speed reached 50 km h^{-1} and the average speed was about 20 km h^{-1}. Vehicle exhaust was sampled into a Summa canister (Entech Inst., USA) during the whole driving cycle. We also collected the samples of gasoline vapor at 4 gas stations in Shanghai to analyze the VOC species of non-tailpipe gasoline.

Concentration of individual VOC in samples was determined by a GC–MS system (Agilent 7890A/5975C) with standard gases prepared by Spectra Gas. The samples collected in the Summa canister were pre-concentrated to an acceptable level for the analytical devices using a 7100A pre-concentrator (Entech Inst., USA) with an Entech 7016CA automatic sample injector. A 50 mL sample was extracted by the preconcentrator into a 1/4 inch liquid nitrogen cold trap to remove water and CO_2, and then separated by GC and detected by MS. The carrier gas was helium.

2.2 Vehicular emission inventory

2.2.1 Road traffic data survey

We developed emission inventories for the pollutants including VOCs, CO, EC, and OC with the IVE model for Shanghai, China. The methodology of the model has been introduced by Wang et al. (2008). Vehicle kilometers of travel (VKT), driving pattern, and fleet composition of several vehicle types were determined with a survey from transportation department in Shanghai in 2012. Annual VKTs were refined into 3 road types, and 7 vehicle categories for Shanghai. The road types include highway, arterial road, and residential road. The vehicle categories include light-duty car, light-duty truck, taxi, heavy-duty bus, heavy-duty truck, city bus, and motorcycle. The distributions of each

ACPD
15, 7977–8015, 2015

vehicle type in the traffic flows were surveyed on various road types with video cameras from March to May. About 4000 valid hours were obtained on 15 road sectors of various road types. Survey days include weekdays and weekends and each day covers 24 h. Light-duty cars are the major vehicle type on the road, accounting for 66, 51, and 47 % of the total flows on highway, arterial road, and residential road respectively. Next are taxis, which account for 7, 14, and 23 % of the total flows. Simultaneously, we installed GPS units on light-duty cars, taxis, buses, and heavy-duty trucks to measure the driving patterns of various vehicle types. About 150 h of valid GPS data were collected. The data covered 2831 km of roads and were composed of 3 road types and 4 vehicle types. Table 2 shows the daily VKT and average speeds of various vehicle and road types in 2012.

2.2.2 Fleet composition data survey

Fleet composition data were collected from the vehicle information database of the Vehicle Management Department of Public Security Bureau of Shanghai. Each vehicle type was classified by fuel type, engine size, and emission standard. Given that the real-world vehicle occurrence frequency is different than the static fleet database, we surveyed almost 30 thousand vehicles including light-duty car, light-duty truck, heavy-duty bus, and heavy-duty truck at 4 inspection stations. Information on vehicle type, license number, model year, and odometer readings were collected for each vehicle. The results indicate that the annual average mileages tend to decrease with the increase in age. The fleet compositions were then adjusted based on their occurrence frequencies. Shanghai implemented the Euro 1 emission standard in 1999 and upgrades the emission standards every 3 to 4 years. By 2012, new registered vehicles are required to meet the Euro 4 emission standard. The results show that Euro 2 vehicles are the major types of light-duty cars and light-duty trucks, accounting for 51 and 68 % respectively. Heavy-duty buses and trucks are mainly composed by Euro 2 and Euro 3 diesel vehicles, accounting for 40 and 45 % respectively. Figure 1 shows the static and adjusted fraction by the vehicle fleet in Shanghai.

ACPD
15, 7977–8015, 2015

2.2.3 Vehicle emission factors

Vehicle emission factors were calculated with the IVE model and adjusted by the results of real-world emission measurements in major cities of China. The calculated emission factors of each vehicle type and the real-world test data are shown in Fig. 2. The test data were collected from real-world vehicle emission measurement studies in major Chinese cities, including Shanghai, Beijing, Guangzhou, Xi'an, Shenzhen, Jinan, and Yichang (Chen et al., 2007; Huo et al., 2012a, b; Wu et al., 2012; Huang et al., 2013). The measurements were all conducted with a Portable Emission Measurement System (PEMS). The emission factors of each vehicle type generally fit well with the measurement results. For LDGVs, VOCs and $PM_{2.5}$ emission factors are slightly higher than the measurement results. For HDDTs, only $PM_{2.5}$ is slightly higher than the measurement data. Limited number of measurements made it difficult to verify the accuracies of the emission factors.

2.3 Air pollution observation

To analyze the contribution of vehicle emissions to SOA in the atmosphere, we utilized the online air pollution observation data from a monitoring site on the roof of a 5-floor building (15 m high above the ground) at Shanghai Academy of Environmental Science (31.17° N, 121.43° E), which is located southwest of urban area of Shanghai. The site is mostly surrounded by commercial properties and residential dwellings. Vehicle exhaust is a major source of pollutants near this site. Carbon monoxide was continuously measured by an ECOTECH EC9820 CO analyzer. $PM_{2.5}$ concentration was measured by a Thermo Fisher commercial instrument β-ray particulate monitor. Organic carbon (OC) and elemental carbon (EC) were measured by a carbon analyzer (model RT-4, Sunset Laboratory Inc.). Water soluble ions were measured by a commercial instrument for online monitoring of aerosols and gases (MARGA, model ADI 2080, Applikon Analytical B.V.). Individual VOC species were continuously measured every 30 min by two on-line gas chromatographs with flame ionization detector (GC-FID) sys-

ACPD
15, 7977–8015, 2015

tems (Chromato-sud airmoVOC C2–C6 #5250308 and airmoVOC C6–C12 #2260308, France).

3 Results and discussion

3.1 VOC species of vehicle emissions and gas evaporation

Figure 3 compares the VOC compositions of the exhausts from different vehicle types and gas evaporation in this study to the results from other countries or regions. To compare the VOC compositions of the exhausts from different types of vehicles, we selected their common species such as C2–C12 alkanes, alkenes, alkynes, and single-ring aromatics, and normalized the concentrations of carbon. The weighted percentages of individual VOC for the exhausts from different vehicle types and gas evaporation were listed in Table S1.

The exhausts from gasoline vehicles (including LDGVs and taxis) had similar VOC compositions. Single-ring aromatics were the major species of the exhausts from gasoline vehicles, accounting for 50 % of the total VOCs approximately. Straight-chain alkanes, branched alkanes, and cycloalkanes comprised 17.0, 18.1, and 6.1 % of the total VOCs, respectively. Toluene, m, p-xylene, o-xylene, and ethylbenzene were the main compounds in LDGV and taxi exhausts, accounting for 7.54, 6.71, 5.20, and 4.42 % of the total VOCs, respectively. Motorcycle emitted more branched alkanes and less single-ring aromatics than LDGVs and taxis. 2-methylhexane (23.43 %) was the most abundant VOC in motorcycle exhausts, followed by m, p-xylene (9.34 %), ethylbenzene (5.53 %) and o-xylene (4.37 %). It was indicated from Fig. 3 that the proportion of single-ring aromatics in LDGV exhausts were higher and the proportion of alkene were lower in this and previous studies in China (Liu et al., 2008; Wang et al., 2013) than those in Hong Kong (Guo et al., 2011) and US (Schauer et al., 2002; Gentner et al., 2013; May et al., 2014). The differences of aromatic content in gasoline fuel in different regions and countries could be the main reason of the difference in the proportion of

ACPD
15, 7977–8015, 2015

aromatic compounds in LDGV exhausts. The limit of aromatic content in current gasoline standard in China was 40 vol%, which was much higher than the limits of gasoline standards of the US (22–25 vol%) and Europe (35 vol%).

High proportion of straight-chain alkanes were measured in the exhausts from diesel vehicles, which accounted for 34.9 and 35.6 % of the total VOCs from HDDT and bus exhausts, respectively. N-dodecane, propene, n-undecane, acetone, and n-decane were major species in diesel exhausts, accounting for 13.65, 10.85, 8.69, 7.00, and 6.86 % of the total VOCs, respectively. The proportions of straight-chain alkanes in diesel exhausts in this study were much higher than those in the previous studies of the US (Schauer et al., 1999; May et al., 2014). Incomplete combustion of diesel fuel caused by poor engine maintenance could be the main reason for the high straight-chain alkane emissions.

High proportion of alkenes was measured in gas evaporation in this study, which accounted for 40 % of the total VOCs. Propane, isopentane, isobutene, 1-pentene, and n-butane were major species in gas evaporation emissions, accounting for 15.99, 11.87, 9.69, 8.87, and 6.51 % of the total VOCs, respectively. The proportions of VOC species in gas evaporation in this study was close to the results in the other study of China (Zhang et al., 2013), but different from the studies in the US (Harley et al., 2000) and Korea (Na et al., 2004), which reported less alkenes and more branched alkanes in gas evaporation.

3.2 SOA yield of different vehicle types and gas evaporation

VOC species of vehicle emissions and gas evaporation were classified into 6 categories by their chemical classes, and their distributions of carbon numbers were shown in Fig. 4a. The carbon numbers of VOCs in gasoline and motorcycle exhausts mainly concentrated in the intervals between C6 to C9. Comparatively, exhausts from diesel vehicles had a wider distribution of carbon number, ranging from C2 to C20. Due to the limitations of analytical method, some alkanes and polycyclic aromatics with large carbon number were not detected in this study. The carbon numbers of VOCs in gas evap-

ACPD
15, 7977–8015, 2015

oration were mainly distributed within the range of C3–C7, which were much smaller than those in the exhausts from different vehicle types.

Figure 4b shows the SOA mass yields of VOC emissions from different vehicle types and gas evaporation and the contributions of chemical classes to the yields. SOA mass yield was the product of the yield of individual VOC species and its mass fraction. The SOA mass yield of each individual VOC species was taken from Gentner et al. (2012), which estimated the SOA mass yields for pure gasoline and diesel fuel using a combination of measured SOA mass yields derived from laboratory-chamber experiments and approximate SOA mass yields based on box modeling. Here we substituted the VOC species in the exhausts for those from pure gasoline and diesel fuel. The SOA mass yield of diesel exhaust reached 0.070, which was the highest among the yields of different vehicle exhausts and gas evaporation. Polycyclic aromatics were the largest contributors to the SOA mass yield of diesel exhaust, which contributed 44 % of the total yield. Next were single-ring aromatics and straight-chain alkanes, contributing 24 % for each. The SOA mass yields of gasoline and motorcycle exhausts were 0.039 and 0.020. Single-ring aromatics were major contributors to their SOA yields, which contributed 92 and 85 %, respectively. Although there were few polycyclic aromatics in gasoline and motorcycle exhausts, these compounds contributed 7 and 15 % of the total yields. The SOA yield of gas evaporation was 0.0005, which was much smaller than those of the vehicle exhausts.

Gordon et al. (2014a) investigated the SOA productions of the exhausts from 15 light-duty gasoline vehicles (including pre-LEV, LEV1, and LEV2) using a smog chamber. The average SOA mass yield of LDGV exhausts was 0.032 ± 0.033. Kleindienst et al. (2011) estimated the SOA mass yield was about 0.020 ± 0.005 according to another smog chamber experiment on a light-duty gasoline vehicle. The calculated yield of gasoline exhaust in this study was slightly larger than the experimental results above. However, given the relatively larger proportion of single-ring aromatics in gasoline exhaust in the studies of China, the SOA yield of gasoline exhausts in this study is considered reasonable. Gordon et al. (2013) reported the average SOA mass yield of 2-

ACPD
15, 7977–8015, 2015

and 4-stroke off-road engine exhausts was 0.031 ± 0.011, which was larger than the calculated SOA yield of motorcycle exhaust in this study. Gordon et al. (2014b) also investigated the SOA productions of diesel exhausts from 2 medium-duty diesel vehicles and 3 heavy-duty diesel vehicles using a smog chamber. The average SOA mass yield of the experiments under UDDS (Urban Dynamometer Driving Schedule) driving cycle was about 0.086 ± 0.025, which was 20 % higher than the calculated result in this study. The possible explanation for this discrepancy is that some semi-volatile organic compounds (SVOCs) and intermediate- volatile organic compounds (IVOCs) larger than C12 were missed in this study due to the limitation of analytic method.

The smog chamber experiments mentioned above were all conducted under high-NO_x conditions. However, Ng et al. (2007) reported higher SOA yields for benzene, toluene, and m-xylene under low-NO_x conditions and considered that low-NO_x conditions were more realistic in the atmosphere. Figure 4c shows the adjusted SOA yields under low-NO_x conditions. The yields of benzene, toluene, m-xylene, naphthalene, and methylnaphthalene were directly adopted from Ng et al. (2007) and Chan et al. (2009). The yields of other species of single-ring aromatics and polycyclic aromatics were derived from the corresponding ratios of low-NO_x to High-NO_x yields of the reported species. The adjusted yields of gasoline, diesel, motorcycle exhausts and gas evaporation under low-NO_x conditions increased to 0.200, 0.186, 0.106, and 0.002, respectively. The contribution of single-ring aromatics to SOA mass increased after the adjustment, especially in the case of diesel exhaust.

3.3 Vehicle emission inventory and SOA formation potentials

Table 3 indicates the emission inventory and their SOA formation potentials of different vehicle and fuel types in Shanghai. The emissions of CO, NO_x, VOCs, EVA (gas evaporation), EC, and POA (OC · 1.2) were 343.9, 110.9, 39.4, 8.9, 4.0, and 4.3 thousand t in Shanghai in 2012. Gasoline vehicles (including LDGV, Taxi, HDGV, and Motorcycle) were the major source of CO, VOCs, and EVA emissions, accounting for 91, 69, and 100 % of the emissions of the pollutants. Diesel vehicles (including LDDV, HDDV, and

ACPD
15, 7977–8015, 2015

Bus) were the major source of NO_x, EC, and POA emissions, comprising 82, 99, and 96 % of the emissions. SOA formation potential was calculated by multiplying the VOC and EVA emission to the SOA mass yield of each vehicle type. High-NO_x and low-NO_x conditions were both considered. Under High-NO_x condition, the SOA formation potential was approximately 1.8 thousand t, about 43 % of the POA emission. Gasoline and diesel vehicles contributed 54 and 46 % of the total SOA formation potential, respectively. LDGV and HDDV were the major vehicle types who contributed 42 and 24 % of the total SOA formation potential. Under low-NO_x condition, the SOA formation potential reached 7.4 thousand t, about 1.7 times the POA emission. The SOA formation potentials from gasoline and diesel vehicles accounted for 69 and 31 %, respectively. LDGV was the major source of SOA formation in low-NO_x condition, contributing 42 % to the total vehicular SOA formation. Next were HDDV and taxi, accounting for 24 and 16 %, respetively.

Figure 5 shows the POA emissions and SOA formation potentials from gasoline and diesel vehicles in Shanghai. When SOA formation potential was taken into account, the contribution of gasoline vehicle to the total OA increased from 4 to 19 % under high-NO_x conditions and 45 % under low-NO_x conditions, respectively. Although gasoline vehicles contributed less to POA emission than diesel ones, their potential impact on organic aerosol formation cannot be ignored. The emission ratio of vehicular POA ($\Delta POA/\Delta CO$) was 15.6 $\mu g\,m^{-3}\,ppmv^{-1}$ according to the emission inventory. The OA production rates ($\Delta OA/\Delta CO$) after photochemical evolution were 22.3 and 42.7 $\mu g\,m^{-3}\,ppmv^{-1}$ under high-NO_x and low-NO_x conditions, respectively.

3.4 Initial emission ratio and SOA formation potential based on observation

Figure S1 shows the time series data of meteorological parameters and concentrations of major air pollutants observed in urban Shanghai in summer (August in 2013) and winter (January in 2013). SOA formation in the urban atmosphere was characterized by a photochemical-age-based parameterization method, developed by de Gouw et al. (2005, 2008). The photochemical age was calculated by the ratio of two VOC

ACPD
15, 7977–8015, 2015

species. In this study, we selected m, p-xylene/ethylbenzene as the clock of photochemical age. The concentrations of m, p-xylene and ethylbenzene showed good correlations during the observation, as shown in Fig. S2, which implied the same source for these two species. The different diurnal variations of m, p-xylene and ethylbenzene indicated that they are engaged in different chemical reactions in the daytime (Fig. S3). Significant depletion of m, p-xylene relative to ethylbenzene was observed in the daytime both in Summer and in Winter.

A photochemical exposure time ($\Delta t \cdot [\mathrm{OH}]$) was calculated based on the ratios of m, p-xylene to ethylbenzene using Eq. (1).

$$\Delta t \cdot [\mathrm{OH}] = \frac{1}{(k_\mathrm{X} - k_\mathrm{E})} \times \left[\ln \left(\frac{[\mathrm{X}]}{[\mathrm{E}]} \bigg|_{t=0} \right) - \ln \left(\frac{[\mathrm{X}]}{[\mathrm{E}]} \right) \right] \quad (1)$$

Here, Δt is photochemical age (h). [OH] is the average OH radical concentrations (molecules cm^{-3}). k_X and k_E are the OH rate constants of m, p-xylene ($18.9 \times 10^{-12}\,\mathrm{cm}^3\,\mathrm{molecule}^{-1}\,\mathrm{s}^{-1}$) and ethylbenzene ($7.0 \times 10^{-12}\,\mathrm{cm}^3\,\mathrm{molecule}^{-1}\,\mathrm{s}^{-1}$). $[\mathrm{X}]/[\mathrm{E}]|_{t=0}$ and [X]/[E] are initial emission ratio and the ratio after photochemical reaction of m, p-xylene to ethylbenzene. Figure 6 illustrates the diurnal distributions of the ratios of observed m, p-xylene to ethylbenzene in summer and winter of 2013. The initial emission ratios of m, p-xylene to ethylbenzene were calculated based on 97.5 % iles of the X/E ratio in summer and winter, which were 2.17 and 1.68, respectively. According to the vehicular emission inventory, the emission ratio of m, p-xylene to ethylbenzene from vehicle exhaust and gas evaporation was about 1.70. The inventory-based vehicular X/E was slightly lower than the initial X/E observed in summer. There could be some other higher X/E emission sources in addition to vehicles. Further research is needed to determine the actual cause.

Figure 7 is a scatterplot of OA vs. CO concentrations measured in urban Shanghai in the summer and the winter of 2013. The observation data were color-coded by the photochemical exposure time ($\Delta t \cdot [\mathrm{OH}]$) determined by Eq. (1). It was indicated from the figure that the ratios of OA to CO concentrations generally showed growing trends

ACPD
15, 7977–8015, 2015

with the increase of the photochemical exposure time both in the summer and winter. The results were similar to the previous studies in the United States, Japan, and Mexico (Bahreini et al., 2012; de Gouw et al., 2008; Takegawa et al., 2006; DeCarlo et al., 2008). Vehicular POA/CO ratio (15.6 $\mu g\,m^{-3}\,ppmv^{-1}$) derived from the vehicular emission inventory was shown with the dotted pink line and was consistent with the primary urban emissions (the ratios of OA to CO concentrations under less photochemical exposure time) observed both in the summer and in the winter. However, the initial emission ratio of vehicular POA to total CO emission (4.34 $\mu g\,m^{-3}\,ppmv^{-1}$) was much lower as shown by the dotted grey line. Total amount of CO emission was 1236.1 t for the whole city. Vehicles accounted for 27.8 % of the total. Detailed information is shown in Fig. S4. The result implies there are other POA emission sources in addition to vehicles in Shanghai. Vehicle emissions only contribute about 25 % to the total POA emission according to the observed minimum $\Delta OA/\Delta CO$ ratio. The ratios of vehicular primary emissions plus secondary formation to vehicular CO emission (11.9 $\mu g\,m^{-3}\,ppmv^{-1}$) under low-NO_x conditions were shown with a dotted red line and the ratios to the total CO emission (42.8 $\mu g\,m^{-3}\,ppmv^{-1}$) was shown with a dotted black line, respectively. The results show that the vehicular primary emissions plus secondary formation ratio was far from enough to explain the organic aerosol pollution in the two seasons of Shanghai when total CO emission was taken into account. Other sources with higher SOA formation potential in addition to vehicles should be responsible for more OA production. Another possible reason is that IVOCs and SVOCs emitted from vehicles, which are not measured in this study, play more important roles in SOA formation as discussed by Zhao et al. (2014).

3.5 Estimation of vehicular SOA contribution in the urban atmosphere

Figure 8 shows the diurnal variations of $\Delta OA/\Delta CO$ ratios observed at the monitoring site and calculated photochemical exposure time ($\Delta t \cdot [OH]$) based on the hourly m, p-xylene to ethylbenzene ratios by Eq. (1) in the summer and the winter of 2013 in urban Shanghai. It can be seen in Fig. 8 that the formation of SOA is strongly dependent on its

ACPD
15, 7977–8015, 2015

photochemical exposure. The average $\Delta t \cdot$[OH] was about 1.6×10^7 molecules cm^{-3} h in the summer. In the role of photochemical reactions, the ΔOA/ΔCO ratio showed rapid growth in the afternoon in the summer and reached a peak around 12:00 LT. Compared to the summer, the photochemical reaction in the winter was relatively weak. The average $\Delta t \cdot$[OH] was only 1.0×10^7 molecules cm^{-3} h. Correspondingly, the ΔOA/ΔCO ratio was significantly lower in the winter than that in the summer and no peak was observed.

To estimate the SOA contribution from vehicle emissions, we calculated the ratios of vehicular POA emissions and OA formation ratios to total CO emissions in Shanghai. The evolution of POA emission and SOA formation was explained by Eq. (2) (de Gouw et al., 2008). POA emission and SOA formation and their loss terms were expressed by the first and second parts in Eq. (2), respectively.

$$\begin{aligned}\frac{\Delta \mathrm{OA}}{\Delta \mathrm{CO}} &= \frac{\Delta \mathrm{POA}}{\Delta \mathrm{CO}} + \frac{\Delta \mathrm{SOA}}{\Delta \mathrm{CO}} \\ &= \mathrm{ER}_{\mathrm{POA}} \times \exp(-L_{\mathrm{OA}} \cdot \Delta t) + \mathrm{ER}_{\mathrm{VOC}_i} \times Y_{\mathrm{OA}_i} \times \frac{P_{\mathrm{OA}}}{L_{\mathrm{OA}} - P_{\mathrm{OA}}} \\ &\quad \times [\exp(-P_{\mathrm{OA}} \cdot \Delta t) - \exp(-L_{\mathrm{OA}} \cdot \Delta t)] \end{aligned} \quad (2)$$

Here, ΔOA/ΔCO is the ratio of vehicular OA formation vs. total CO emission after photochemical reaction $\mathrm{ER}_{\mathrm{POA}}$ is the initial emission ratio of vehicular POA to total CO emission. $\mathrm{ER}_{\mathrm{VOC}_i}$ are the initial emission ratios of VOC from vehicle type i to total CO emission in the unit of ppbv^{-1} ppmv^{-1}. Y_{OA_i} is the yield of VOC species from vehicle type i to produce OA under low-$\mathrm{NO_x}$ condition. L_{OA} and P_{OA} are the loss and formation rate of organic aerosol, respectively. We used the empirical parameters derived by de Gouw et al. (2008), which were 0.00677 and 0.0384 h^{-1}, respectively. Δt is the photochemical age calculated by Eq. (1) in each hour.

The average ratios of vehicular POA and SOA to total CO were 4.19 and 1.37 µg m^{-3} ppmv^{-1} in the summer, 4.25 and 0.90 µg m^{-3} ppmv^{-1} in the winter. The

ACPD
15, 7977–8015, 2015

SOA formation ratios of vehicles accounted for 25 and 18 % of the total vehicular OA formation ratios in the summer and winter, respectively. However, the maximum SOA formation potential from vehicle emissions when VOCs were completely removed could reach 63 % of the total vehicular OA mass, as shown in Fig. 5. The main reason for the difference above was the monitoring site in this studywas located in an urban area, where the air mass was much closer to fresh emission and the reaction of VOCs was not complete.

The vehicular OA mass accounted for 15 and 22 % of the total organic aerosols observed in the summer and winter, respectively. The results imply that (1) vehicles contribute more organic aerosols in the winter than in the summer; (2) there are other emission sources with higher SOA formation potentials in addition to vehicles in Shanghai; or (3) the unmeasured IVOCs and SVOCs from vehicles may contribute more SOA formation than expected.

3.6 SOA formation contribution of different vehicle types

Figure 9 shows the changes of OA formation ratios of vehicle emissions in different vehicle types (see Fig. 9a) and fuel types (see Fig. 9b) with the increase of the photochemical age. The OA formation ratios were calculated based on the initial POA and VOCs emission ratios and SOA mass yields of different types of vehicles under low-NO_x condition according to Eq. (2). The vehicular $\Delta OA/\Delta CO$ ratio showed a rapid growth trend with the photochemical ages in the first 30 h and then stabilized. Gasoline vehicles (including LDGV, taxi, HDGV, and motorcycle) showed a much higher growth rate of $\Delta OA/\Delta CO$ ratios than diesel vehicles (including LDDV, HDDV, and bus). The initial POA emission of gasoline vehicles accounted for 4 % of the total POA emission. Their contributions increased to 21 % after 6 h and 38 % after 24 h of photochemical aging. HDDV and LDGV were major contributors of vehicular OA formation, accounting for 50 and 23 % of the total in the scenario of 24 h photochemical aging.

ACPD
15, 7977–8015, 2015

4 Conclusions

We measured the VOC species in the exhausts from different vehicle types and gas evaporation in Shanghai, China and estimated the SOA formation potentials of each vehicle type and gas evaporation based on the emission and SOA yield of the individual VOC species. The calculated SOA mass yields of the emissions from different vehicle types were close to the experimental results from the smog chamber in the previous studies with the exception of that of diesel exhaust, which was 20 % lower than the experimental data. Absence of SVOCs and LVOCs measurement on diesel exhaust could be the main reason for the under estimation. The vehicular POA emission ratio ($\Delta POA/\Delta CO$) of Shanghai was about 15.6 $\mu g\,m^{-3}\,ppmv^{-1}$ based on the vehicular emission inventory. The vehicular OA production rates ($\Delta OA/\Delta CO$) were 22.3 and 42.7 $\mu g\,m^{-3}\,ppmv^{-1}$, about 40 and 170 % times higher than POA emission ratio under high-NO_x and low-NO_x conditions, respectively. To estimate the contribution of vehicular POA emission and SOA formation to organic aerosol pollution in urban Shanghai, we calculated the vehicular OA production ratio with a photochemical-age-based parameterization method and compared the ratio with the observation data from an urban atmospheric environmental monitoring site. The results showed that SOA formations from vehicular VOCs emissions could explain 15 and 22 % of total organic aerosols observed in the summer and winter in urban Shanghai, respectively. SOA production accounted for 25 and 18 % of the total vehicular OA formation in the summer and winter since the reaction of VOCs was not complete in the urban atmosphere. The contribution of gasoline exhausts to OA formation showed a rapid growth trend with the increase of photochemical age. The proportions of the $\Delta OA/\Delta CO$ ratio from gasoline vehicle were 4, 21, 30, and 38 % after 0, 6, 12, and 24 h of photochemical aging.

There are some uncertainties in the main findings of this study. First is the SOA mass yield. Since the absence of SVOCs and IVOCs measurement on vehicle exhausts, the calculated SOA mass yield may be underestimated. For example, the calculated SOA mass yield of diesel exhaust was 20 % lower than the smog chamber experiment re-

ACPD
15, 7977–8015, 2015

sult. The vehicular OA production would increase 2 % if we used the SOA yield of diesel exhaust from the smog chamber experiment. Emission inventory is another important source of uncertainty in this study. To reduce the uncertainty of vehicular emission inventory, we adjusted the vehicle mileage and emission factor data based on local surveys in Shanghai and real-world measurements in some cities of China. However, the CO emission inventories of other sources shown in Fig. S4 still have large uncertainties according to the previous study (Huang et al., 2011). More accurate emission inventory will be helpful to reduce the uncertainty of vehicular OA contribution in this study.

Huang et al. (2014) has reported the fossil OA was a dominant fraction of OA mass (about 25–40 %) in Shanghai and Beijing based on the observation data. Traffic and coal burning were major sources of the fossil OA. Our result of vehicular OA formation contribution (about 15–22 %) was in that range. No further studies distinguished between the SOA contributions from vehicle and coal burning. However, it can be concluded that there must be other contributors (e.g. coal burning, biomass burning, cooking, dust, etc.) to OA pollution in addition to vehicles in urban Shanghai. Another implication in this study is that the potential role of IVOCs and SVOCs in vehicle exhausts may be very important on the SOA formation. Therefore, further studies need to be conducted to determine the contributions of different sources and IVOCs and SVOCs emissions to OA pollution in China.

The Supplement related to this article is available online at doi:10.5194/acpd-15-7977-2015-supplement.

Acknowledgements. This study was supported by the National Key Technology R&D Program via grant No. 2014BAC22B03, the National Natural Science Foundation of China (NSFC) via grant No. 41205122, the National Environmental Public Welfare Research Program of Ministry of Environmental Protection of China via grant No. 201409008, the Science and Technol-

ACPD
15, 7977–8015, 2015

ogy Commission of Shanghai Municipality Fund Project via grant No. 14DZ1202905, and the Shanghai Natural Science Foundation via grant No. 15ZR1434700.

References

Bahreini, R., Middlebrook, A. M., de Gouw, J. A., Warneke, C., Trainer, M., Brock, C. A., Stark, H., Brown, S. S., Dube, W. P., Gilman, J. B., Hall, K., Holloway, J. S., Kuster, W. C., Perring, A. E., Prévôt, A. S. H., Schwarz, J. P., Spackman, J. R., Szidat, S., Wagner, N. L., Weber, R. J., Zotter, P., and Parrish, D. D.: Gasoline emissions dominate over diesel in formation of secondary organic aerosol mass, Geophys. Res. Lett., 39, L06805, doi:10.1029/2011GL050718, 2012.

Borbon, A., Gilman, J. B., Kuster, W. C., Grand, N., Chevaillier, S., Colomb, A., Dolgorouky, C., Gros, V., Lopez, M., Sarda-Esteve, R., Holloway, J., Stutz, J., Petetin, H., McKeen, S., Beekmann, M., Warneke, C., Parrish, D. D., and de Gouw, J. A.: Emission ratios of anthropogenic volatile organic compounds in northern mid-latitude megacities: observations versus emission inventories in Los Angeles and Paris, J. Geophys. Res.-Atmos., 118, 2041–2057, doi:10.1002/jgrd.50059, 2013.

Cai, C. J., Geng, F. H., Tie, X. X., Yu, Q., and An, J. L.: Characteristics and source apportionment of VOCs measured in Shanghai, China, Atmos. Environ., 44, 5005–5014, 2010.

Cao, J.-J., Zhu, C.-S., Tie, X.-X., Geng, F.-H., Xu, H.-M., Ho, S. S. H., Wang, G.-H., Han, Y.-M., and Ho, K.-F.: Characteristics and sources of carbonaceous aerosols from Shanghai, China, Atmos. Chem. Phys., 13, 803–817, doi:10.5194/acp-13-803-2013, 2013.

Chan, A. W. H., Kautzman, K. E., Chhabra, P. S., Surratt, J. D., Chan, M. N., Crounse, J. D., Kürten, A., Wennberg, P. O., Flagan, R. C., and Seinfeld, J. H.: Secondary organic aerosol formation from photooxidation of naphthalene and alkylnaphthalenes: implications for oxidation of intermediate volatility organic compounds (IVOCs), Atmos. Chem. Phys., 9, 3049–3060, doi:10.5194/acp-9-3049-2009, 2009.

Chen, C. H., Huang, C., Jing, Q. G., Wang, H. K., Pan, H. S., Li, L., Zhao, J., Dai, Y., Huang, H. Y., Schipper, L., and Streets, D. G.: On-road emission characteristics of heavy-duty diesel vehicles in Shanghai, Atmos. Environ., 41, 5334–5344, 2007.

Chirico, R., DeCarlo, P. F., Heringa, M. F., Tritscher, T., Richter, R., Prévôt, A. S. H., Dommen, J., Weingartner, E., Wehrle, G., Gysel, M., Laborde, M., and Baltensperger, U.: Impact

ACPD
15, 7977–8015, 2015

of aftertreatment devices on primary emissions and secondary organic aerosol formation potential from in-use diesel vehicles: results from smog chamber experiments, Atmos. Chem. Phys., 10, 11545–11563, doi:10.5194/acp-10-11545-2010, 2010.

DeCarlo, P. F., Dunlea, E. J., Kimmel, J. R., Aiken, A. C., Sueper, D., Crounse, J., Wennberg, P. O., Emmons, L., Shinozuka, Y., Clarke, A., Zhou, J., Tomlinson, J., Collins, D. R., Knapp, D., Weinheimer, A. J., Montzka, D. D., Campos, T., and Jimenez, J. L.: Fast airborne aerosol size and chemistry measurements above Mexico City and Central Mexico during the MILAGRO campaign, Atmos. Chem. Phys., 8, 4027–4048, doi:10.5194/acp-8-4027-2008, 2008.

de Gouw, J. and Jimenez, J. L.: Organic aerosols in the Earth's atmosphere, Environ. Sci. Technol., 43, 7614–7618, 2009.

de Gouw, J. A., Middlebrook, A. M., Warneke, C., Goldan, P. D., Kuster, W. C., Roberts, J. M., Fehsenfeld, F. C., Worsnop, D. R., Canagaratna, M. R., Pszenny, A. A. P., Keene, W. C., Marewka, M., Bertman, S. B., and Bates, T. S.: Budget of organic carbon in a polluted atmosphere: results from the New England Air Quality Study in 2002, J. Geophys. Res.-Atmos., 110, D16305, doi:10.1029/2004jd005623, 2005.

de Gouw, J. A., Brock, C. A., Atlas, E. L., Bates, T. S., Fehsenfeld, F. C., Goldan, P. D., Holloway, J. S., Kuster, W. C., Lerner, B. M., Matthew, B. M., Middlebrook, A. M., Onasch, T. B., Peltier, R. E., Quinn, P. K., Senff, C. J., Stohl, A., Sullivan, A. P., Trainer, M., Warneke, C., Weber, R. J., and Williams, E. J.: Sources of particulate matter in the northeastern United States in summer: 1. Direct emissions and secondary formation of organic matter in urban plumes, J. Geophys. Res.-Atmos., 113, D08301, doi:10.1029/2007JD009243, 2008.

Feng, J. L., Chan, C. K., Fang, M., Hu, M., He, L. Y., and Tang, X. Y.: Characteristics of organic matter in $PM_{2.5}$ in Shanghai, Chemosphere, 64, 1393–1400, 2005.

Feng, J. L., Li, M., Zhang, P., Gong, S. Y., Zhong, M., Wu, M. H., Zheng, M., Chen, C. H., Wang, H. L., and Lou, S. R.: Investigation of the sources and seasonal variations of secondary organic aerosols in $PM_{2.5}$ in Shanghai with organic tracers, Atmos. Environ., 79, 614–622, 2013.

Feng, Y. L., Chen, Y. J., Guo, H., Zhi, G. R., Xiong, S. C., Li, J., Sheng, G. Y., and Fu, J. M.: Characteristics of organic and elemental carbon in $PM_{2.5}$ samples in Shanghai, China, Atmos. Res., 92, 434–442, 2009.

Gentner, D. R., Isaacman, G., Worton, D. R., Chan, A. W. H., Dallmann, T. R., Davis, L., Liu, S., Day, D. A., Russell, L. M., Wilson, K. R., Weber, R., Uha, A., Harley, R. A., and

ACPD
15, 7977–8015, 2015

Goldstein, A. H.: Elucidating secondary organic aerosol from diesel and gasoline vehicles through detailed characterization of organic carbon emissions, P. Natl. Acad. Sci. USA, 109, 18318–18323, 2012.

Gentner, D. R., Worton, D. R., Isaacman, G., Davis, L. C., Dallmann, T. R., Wood, E. C., Herndon, S. C., Goldstein, A. H., and Harley, R. A.: Chemical composition of gas-phase organic carbon emissions from motor vehicles and implications for ozone production, Environ. Sci. Technol., 47, 11837–11848, 2013.

Gordon, T. D., Tkacik, D. S., Presto, A. A., Zhang, M., Jathar, S. H., Nguyen, N. T., Massetti, J., Truong, T., Cicero-Fernandez, P., Maddox, C., Rieger, P., Chattopadhyay, S., Maldonado, H., Maricq, M. M., and Robinson, A. L.: Primary gas- and particle-phase emissions and secondary organic aerosol production from gasoline and diesel off-road engines, Environ. Sci. Technol., 47, 14137–14146, 2013.

Gordon, T. D., Presto, A. A., May, A. A., Nguyen, N. T., Lipsky, E. M., Donahue, N. M., Gutierrez, A., Zhang, M., Maddox, C., Rieger, P., Chattopadhyay, S., Maldonado, H., Maricq, M. M., and Robinson, A. L.: Secondary organic aerosol formation exceeds primary particulate matter emissions for light-duty gasoline vehicles, Atmos. Chem. Phys., 14, 4661–4678, doi:10.5194/acp-14-4661-2014, 2014a.

Gordon, T. D., Presto, A. A., Nguyen, N. T., Robertson, W. H., Na, K., Sahay, K. N., Zhang, M., Maddox, C., Rieger, P., Chattopadhyay, S., Maldonado, H., Maricq, M. M., and Robinson, A. L.: Secondary organic aerosol production from diesel vehicle exhaust: impact of aftertreatment, fuel chemistry and driving cycle, Atmos. Chem. Phys., 14, 4643–4659, doi:10.5194/acp-14-4643-2014, 2014b.

Grieshop, A. P., Donahue, N. M., and Robinson, A. L.: Laboratory investigation of photochemical oxidation of organic aerosol from wood fires 2: analysis of aerosol mass spectrometer data, Atmos. Chem. Phys., 9, 2227–2240, doi:10.5194/acp-9-2227-2009, 2009.

Guo, H., Zou, S. C., Tsai, W. Y., Chan, L. Y., and Blake, D. R.: Emission characteristics of nonmethane hydrocarbons from private cars and taxis at different driving speeds in Hong Kong, Atmos. Environ., 45, 2711–2721, 2011.

Hallquist, M., Wenger, J. C., Baltensperger, U., Rudich, Y., Simpson, D., Claeys, M., Dommen, J., Donahue, N. M., George, C., Goldstein, A. H., Hamilton, J. F., Herrmann, H., Hoffmann, T., Iinuma, Y., Jang, M., Jenkin, M. E., Jimenez, J. L., Kiendler-Scharr, A., Maenhaut, W., McFiggans, G., Mentel, Th. F., Monod, A., Prévôt, A. S. H., Seinfeld, J. H., Surratt, J. D., Szmigielski, R., and Wildt, J.: The formation, properties and impact of sec-

ACPD
15, 7977–8015, 2015

ondary organic aerosol: current and emerging issues, Atmos. Chem. Phys., 9, 5155–5236, doi:10.5194/acp-9-5155-2009, 2009.
Harley, R. A., Coulter-Burke, S. C., and Yeung, T. S.: Relating liquid fuel and headspace vapor composition for California reformulated gasoline samples containing ethanol, Environ. Sci. Technol., 34, 4088–4094, 2000.
Hayes, P. L., Ortega, A. M., Cubison, M. J., Froyd, K. D., Zhao, Y., Cliff, S. S., Hu, W. W., Toohey, D. W., Flynn, J. H., Lefer, B. L., Grossberg, N., Alvarez, S., Rappengluck, B., Taylor, J. W., Allan, J. D., Holloway, J. S., Gilman, J. B., Kuster, W. C., de Gouw, J. A., Massoli, P., Zhang, X., Liu, J., Weber, R. J., Corrigan, A. L., Russell, L. M., Isaacman, G., Worton, D. R., Kreisberg, N. M., Goldstein, A. H., Thalman, R., Waxman, E. M., Volkamer, R., Lin, Y. H., Surratt, J. D., Kleindienst, T. E., Offenberg, J. H., Dusanter, S., Griffith, S., Stevens, P. S., Brioude, J., Angevine, W. M., and Jimenez, J. L.: Organic aerosol composition and sources in Pasadena, California during the 2010 CalNex Campaign, J. Geophys. Res.-Atmos., 118, 9233–9257, doi:10.1002/jgrd.50530, 2013.
Hou, B., Zhuang, G. S., Zhang, R., Liu, T. N., Guo, Z. G., and Chen, Y.: The implication of carbonaceous aerosol to the formation of haze: revealed from the characteristics and sources of OC/EC over a mega-city in China, J. Hazard. Mater., 190, 529–536, 2011.
Huang, C., Chen, C. H., Li, L., Cheng, Z., Wang, H. L., Huang, H. Y., Streets, D. G., Wang, Y. J., Zhang, G. F., and Chen, Y. R.: Emission inventory of anthropogenic air pollutants and VOC species in the Yangtze River Delta region, China, Atmos. Chem. Phys., 11, 4105–4120, doi:10.5194/acp-11-4105-2011, 2011.
Huang, C., Lou, D. M., Hu, Z. Y., Feng, Q., Chen, Y. R., Chen, C. H., Tan, P. Q., and Yao, D.: A PEMS study of the emissions of gaseous pollutants and ultrafine particles from gasoline- and diesel-fueled vehicles, Atmos. Environ., 77, 703–710, 2013.
Huang, R. J., Zhang, Y. L., Bozzetti, C., Ho, K. F., Cao, J. J., Han, Y. M., Daellenbach, K. R., Slowik, J. G., Platt, S. M., Canonaco, F., Zotter, P., Wolf, R., Pieber, S. M., Bruns, E. A., Crippa, M., Ciarelli, G., Piazzalunga, A., Schwikowski, M., Abbaszade, G., Schnelle-Kreis, J., Zimmermann, R., An, Z., Szidat, S., Baltensperger, U., El Haddad, I., and Prévôt, A. S. H.: High secondary aerosol contribution to particulate pollution during haze events in China, Nature, 514, 218–222, doi:10.1038/nature13774, 2014.
Huang, X.-F., He, L.-Y., Xue, L., Sun, T.-L., Zeng, L.-W., Gong, Z.-H., Hu, M., and Zhu, T.: Highly time-resolved chemical characterization of atmospheric fine particles during 2010 Shanghai World Expo, Atmos. Chem. Phys., 12, 4897–4907, doi:10.5194/acp-12-4897-2012, 2012.

ACPD
15, 7977–8015, 2015

Huang, X. F., Xue, L., Tian, X. D., Shao, W. W., Sun, T. L., Gong, Z. H., Ju, W. W., Jiang, B., Hu, M., and He, L. Y.: Highly time-resolved carbonaceous aerosol characterization in Yangtze River Delta of China: composition, mixing state and secondary formation, Atmos. Environ., 64, 200–207, 2013.

Hung, H. F. and Wang, C. S.: Formation of secondary organic aerosols and reactive oxygen species from diluted motorcycle exhaust, J. Chin. Inst. Chem. Eng., 37, 491–499, 2006.

Huo, H., Yao, Z. L., Zhang, Y. Z., Shen, X. B., Zhang, Q., Ding, Y., and He, K. B.: On-board measurements of emissions from light-duty gasoline vehicles in three mega-cities of China, Atmos. Environ., 49, 371–377, 2012a.

Huo, H., Yao, Z. L., Zhang, Y. Z., Shen, X. B., Zhang, Q., and He, K. B.: On-board measurements of emissions from diesel trucks in five cities in China, Atmos. Environ., 54, 159–167, 2012b.

Jathar, S. H., Miracolo, M. A., Tkacik, D. S., Donahue, N. M., Adams, P. J., and Robinson, A. L.: Secondary organic aerosol formation from photo-oxidation of unburned fuel: experimental results and implications for aerosol formation from combustion emissions, Environ. Sci. Technol., 47, 12886–12893, 2013.

Jimenez, J. L., Canagaratna, M. R., Donahue, N. M., Prévôt, A. S. H., Zhang Q., Kroll, J. H., DeCarlo, P. F., Allan, J. D., Coe, H., Ng, N. L., Aiken, A. C., Docherty, K. S., Ulbrich, I. M., Grieshop, A. P., Robinson, A. L., Duplissy, J., Smith, J. D., Wilson, K. R., Lanz, V. A., Hueglin, C., Sun, Y. L., Tian, J., Laaksonen, A., Raatikainen, T., Rautiainen, J., Vaattovaara, P., Ehn, M., Kulmala, M., Tomlinson, J. M., Collins, D. R., Cubison, M. J., Dunlea, E. J., Huffman, J. A., Onasch, T. B., Alfarra, M. R., Williams, P. I., Bower, K., Kondo, Y., Schneider, J., Drewnick, F., Borrmann, S., Weimer, S., Demerjian, K., Salcedo, D., Cottrell, L., Griffin,R., Takami, A., Miyoshi, T., Hatakeyama, S.,Shimono, A., Sun, J. Y., Zhang, Y. M., Dzepina, K., Kimmel, J. R., Sueper, D., Jayne, J. T., Herndon, S. C., Trimborn, A. M., Williams, L. R., Wood, E. C., Middlebrook, A. M., Kolb, C. E., Baltensperger, U., Worsnop, D. R.: Evolution of organic aerosols in the atmosphere, Science, 326, 1525–1529, 2009.

Kleindienst, T. E., Corse, E. W., Li, W., McIver, C. D., Conver, T. S., Edney, E. O., Driscoll, D. J., Speer, R. E., Weathers, W. S., and Tejada, S. B.: Secondary organic aerosol formation from the irradiation of simulated automobile exhaust, J. Air Waste Manage., 52, 259–272, 2002.

Liu, S., Ahlm, L., Day, D. A., Russell, L. M., Zhao, Y. L., Gentner, D. R., Weber, R. J., Goldstein, A. H., Jaoui, M., Offenberg, J. H., Kleindienst, T. E., Rubitschun, C., Surratt, J. D., Sheesley, R. J., and Scheller, S.: Secondary organic aerosol formation from fossil fuel

ACPD
15, 7977–8015, 2015

sources contribute majority of summertime organic mass at Bakersfield, J. Geophys. Res.-Atmos., 117, D00V26, doi:10.1029/2012JD018170, 2012

Liu, Y., Shao, M., Fu, L. L., Lu, S. H., Zeng, L. M., and Tang, D. G.: Source profiles of volatile organic compounds (VOCs) measured in China: Part I, Atmos. Environ., 42, 6247–6260, 2008.

May, A. A., Nguyen, N. T., Presto, A. A., Gordon, T. D., Lipsky, E. M., Karve, M., Gutierrez, A., Robertson, W. H., Zhang, M., Brandow, C., Chang, O., Chen, S., Cicero-Fernandez, P., Dinkins, L., Fuentes, M., Huang, S. M., Ling, R., Long, J., Maddox, C., Massetti, J., McCauley, E., Miguel, A., Na, K., Ong, R., Pang, Y., Rieger, P., Sax, T., Truong, T., Vo, T., Chattopadhyay, S., Maldonado, H., Maricq, M. M., and Robinson, A. L.: Gas- and particle-phase primary emissions from in-use, on-road gasoline and diesel vehicles, Atmos. Environ., 88, 247–260, 2014.

Na, K., Kim, Y. P., Moon, I., and Moon, K. C.: Chemical composition of major VOC emission sources in the Seoul atmosphere, Chemosphere, 55, 585–594, 2004.

Ng, N. L., Kroll, J. H., Chan, A. W. H., Chhabra, P. S., Flagan, R. C., and Seinfeld, J. H.: Secondary organic aerosol formation from *m*-xylene, toluene, and benzene, Atmos. Chem. Phys., 7, 3909–3922, doi:10.5194/acp-7-3909-2007, 2007.

Nordin, E. Z., Eriksson, A. C., Roldin, P., Nilsson, P. T., Carlsson, J. E., Kajos, M. K., Hellén, H., Wittbom, C., Rissler, J., Löndahl, J., Swietlicki, E., Svenningsson, B., Bohgard, M., Kulmala, M., Hallquist, M., and Pagels, J. H.: Secondary organic aerosol formation from idling gasoline passenger vehicle emissions investigated in a smog chamber, Atmos. Chem. Phys., 13, 6101–6116, doi:10.5194/acp-13-6101-2013, 2013.

Odum, J. R., Jungkamp, T. P. W., Griffin, R. J., Forstner, H. J. L., Flagan, R. C., and Seinfeld, J. H.: Aromatics, reformulated gasoline, and atmospheric organic aerosol formation, Environ. Sci. Technol., 31, 1890–1897, 1997.

Platt, S. M., El Haddad, I., Zardini, A. A., Clairotte, M., Astorga, C., Wolf, R., Slowik, J. G., Temime-Roussel, B., Marand, N., Ježek, I., Drinovec, L., Močnik, G., Möhler, O., Richter, R., Barmet, P., Bianchi, F., Baltensperger, U., and Prévôt, A. S. H.: Secondary organic aerosol formation from gasoline vehicle emissions in a new mobile environmental reaction chamber, Atmos. Chem. Phys., 13, 9141–9158, doi:10.5194/acp-13-9141-2013, 2013.

Robinson, A. L., Donahue, N. M., Shrivastava, M. K., Weitkamp, E. A., Sage, A. M., Grieshop, A. P., Lane, T. E., Pierce, J. R., and Pandis, S. N.: Rethinking organic aerosols: semivolatile emissions and photochemical aging, Science, 315, 1259–1262, 2007.

ACPD
15, 7977–8015, 2015

SCCTPI (Shanghai City Comprehensive Transportation Planning Institute): Shanghai comprehensive transportation annual report, Shanghai, 2012.
Schauer, J. J., Kleeman, M., Cass, G., and Simoneit, B. T.: Measurement of emissions from air pollution sources. 2. C1 through C30 organic compounds from medium duty diesel trucks, Environ. Sci. Technol., 33, 1578–1587, 1999.
Schauer, J. J., Kleeman, M., Cass, G., and Simoneit, B. T.: Measurement of emissions from air pollution sources. 5. C1–C32 organic compounds from gasoline-powered motor vehicles, Environ. Sci. Technol., 36, 1169–1180, 2002.
Stone, E. A., Zhou, J., Snyder, D. C., Rutter, A. P., Mieritz, M., and Schauer, J. J.: A comparison of summertime secondary organic aerosol source contributions at contrasting urban locations, Environ. Sci. Technol., 43, 3448–3454, 2009.
Takegawa, N., Miyakawa, T., Kondo, Y., Jimenez, J. L., Zhang, Q., Worsnop, D. R., and Fukuda, M.: Seasonal and diurnal variations of submicron organic aerosol in Tokyo observed using the Aerodyne aerosol mass spectrometer, J. Geophys. Res.-Atmos., 111, D11206, doi:10.1029/2005JD006515, 2006.
Wang, H. K., Chen, C. H., Huang, C., and Fu, L. X.: On-road vehicle emission inventory and its uncertainty analysis for Shanghai, China, Sci. Total Environ., 398, 60–67, 2008.
Wang, H. L., Chen, C. H., Wang, Q., Huang, C., Su, L. Y., Huang, H. Y., Lou, S. R., Zhou, M., Li, L., Qiao, L. P., and Wang, Y. H.: Chemical loss of volatile organic compounds and its impact on the source analysis through a two-year continuous measurement, Atmos. Environ., 80, 488–498, 2013.
Wang, J., Jin, L. M., Gao, J. H., Shi, J. W., Zhao, Y. L., Liu, S. X., Jin, T. S., Bai, Z. P., and Wu, C. Y.: Investigation of speciated VOC in gasoline vehicular exhaust under ECE and EUDC test cycles, Sci. Total Environ., 445–446, 110–116, 2013.
Warneke, C., de Gouw, J. A., Goldan, P. D., Kuster, W. C., Williams, E. J., Lerner, B. M., Jakoubek, R., Brown, S. S., Stark, H., Aldener, M., Ravishankara, A. R., Roberts, J. M., Marewka, M., Bertman, S., Sueper, D. T., McKeen, S. A., Meagher, J. F., and Fehsenfeld, F. C.: Comparison of daytime and nighttime oxidation of biogenic and anthropogenic VOCs along the New England coast in summer during New England Air Quality Study 2002, J. Geophys. Res.-Atmos., 109, D10309, doi:10.1029/2003jd004424, 2004.
Weitkamp, E. A., Sage, A. M., Pierce, J. R., Donahue, N. M., and Robinson, A. L.: Organic aerosol formation from photochemical oxidation of diesel exhaust in a smog chamber, Environ. Sci. Technol., 41, 6969–6975, 2007.

ACPD
15, 7977–8015, 2015

Wu, Y., Zhang, S. J., Li, M. L., Ge, Y. S., Shu, J. W., Zhou, Y., Xu, Y. Y., Hu, J. N., Liu, H., Fu, L. X., He, K. B., and Hao, J. M.: The challenge to NO_x emission control for heavy-duty diesel vehicles in China, Atmos. Chem. Phys., 12, 9365–9379, doi:10.5194/acp-12-9365-2012, 2012.

Ye, B. M., Ji, X. L., Yang, H. Z., Yao, X. H., Chan, C. K., Cadle, S. H., Chan, T., and Mulawa, P. A.: Concentration and chemical composition of $PM_{2.5}$ in Shanghai for a 1 year period, Atmos. Environ., 37, 499–510, 2003.

Yuan, B., Hu, W. W., Shao, M., Wang, M., Chen, W. T., Lu, S. H., Zeng, L. M., and Hu, M.: VOC emissions, evolutions and contributions to SOA formation at a receptor site in eastern China, Atmos. Chem. Phys., 13, 8815–8832, doi:10.5194/acp-13-8815-2013, 2013.

Zhang, Y. L., Wang, X. M., Zhang, Z., Lü, S. J., Shao, M., Lee, S. C., and Yu, J. Z.: Species profiles and normalized reactivity of volatile organic compounds from gasoline evaporation in China, Atmos. Environ., 79, 110–118, 2013.

Zhao, Y. L., Hennigan, C. J., May, A. A., Tkacik, D. S., de Gouw, J. A., Gilman, J. B., Kuster, W. C., Borbon, A., and Robinson, A. L.: Intermediate-volatility organic compounds: a large source of secondary organic aerosol, Environ. Sci. Technol., 48, 13743–13750, 2014.

ACPD
15, 7977–8015, 2015

Table 1. Test vehicle specifications.

ID	Vehicle type	Fuel type	Emission standard	Model year	Odometer reading (km)
LDGV-1	Light-duty car	Gasoline	Euro 1	2002	245 306
LDGV-2	Light-duty car	Gasoline	Euro 2	2005	59 790
LDGV-3	Light-duty car	Gasoline	Euro 3	2008	87 662
LDGV-4	Light-duty car	Gasoline	Euro 3	2008	80 856
Taxi-1	Light-duty taxi	Gasoline	Euro 1	2001	270 000
Taxi-2	Light-duty taxi	Gasoline	Euro 1	2002	~ 100 000
Taxi-3	Light-duty taxi	Gasoline	Euro 2	2003	99 638
Taxi-4	Light-duty taxi	Gasoline	Euro 3	2007	281 315
Taxi-5	Light-duty taxi	Gasoline	Euro 3	2008	361 180
HDDT-1	Heavy-duty truck	Diesel	Euro 1	2003	331 387
HDDT-2	Heavy-duty truck	Diesel	Euro 1	2003	271 000
HDDT-3	Heavy-duty truck	Diesel	Euro 2	2004	271 125
HDDT-4	Heavy-duty truck	Diesel	Euro 2	2004	204 193
HDDT-5	Heavy-duty truck	Diesel	Euro 3	2009	70 000
Bus-1	City bus	Diesel	Euro 2	2006	295 236
Bus-2	City bus	Diesel	Euro 3	2006	175 122
MT-1	Motorcycle	Gasoline	Euro 1	2003	15 000
MT-2	Motorcycle	Gasoline	Euro 1	2003	11 191
MT-3	Motorcycle	Gasoline	Euro 2	2004	96 969
MT-4	Motorcycle	Gasoline	Euro 2	2003	13 912
MT-5	Motorcycle	Gasoline	Euro 2	2003	5379

ACPD
15, 7977–8015, 2015

Table 2. Daily VKT and average speeds of various vehicle and road types in Shanghai in 2012.

Road types	Daily vehicle kilometers traveled (million km)								
	Light-duty car	Light-duty truck	Taxi	Heavy-duty bus	Heavy-duty truck	City bus	Motor-cycle	Total	Average speed ($km\,h^{-1}$)
Highway	38.3	0.62	3.96	3.10	11.82	0.23	0.00	58.04	57.9
Arterial road	22.6	2.93	6.16	1.12	4.73	1.58	5.29	44.41	36.0
Residential road	18.3	3.11	8.92	0.89	1.90	1.38	4.15	38.64	28.5
Total	79.2	6.66	19.04	5.11	18.45	3.19	9.44	141.09	43.0

ACPD
15, 7977–8015, 2015

Table 3. Vehicle emission inventory and SOA formation potential in Shanghai.

Vehicle type	Emission inventory (kt)						SOA formation potential (kt)	
	CO	NO_x	VOCs	EVA	EC	POA (OC·1.2)	High-NO_x	Low-NO_x
in vehicle type								
LDGV	192.03	13.30	15.59	6.15	0.02	0.07	0.60	3.13
LDDV	1.89	5.72	0.32	0.00	0.17	0.11	0.02	0.06
Taxi	68.89	3.86	5.56	1.96	0.01	0.03	0.22	1.16
HDGV	36.79	2.20	2.29	0.29	0.00	0.01	0.09	0.46
HDDV	24.71	67.56	9.74	0.00	3.16	3.40	0.68	1.82
Bus	5.53	17.56	2.06	0.00	0.58	0.62	0.15	0.43
Motorcycle	14.01	0.67	3.85	0.49	0.02	0.06	0.08	0.41
in fuel type								
Gasoline	311.71	20.04	27.28	8.88	0.05	0.17	0.99	5.16
Diesel	32.14	90.84	12.12	0.00	3.91	4.13	0.85	2.31
Total	343.85	110.88	39.40	8.88	3.96	4.30	1.84	7.46

ACPD
15, 7977–8015, 2015

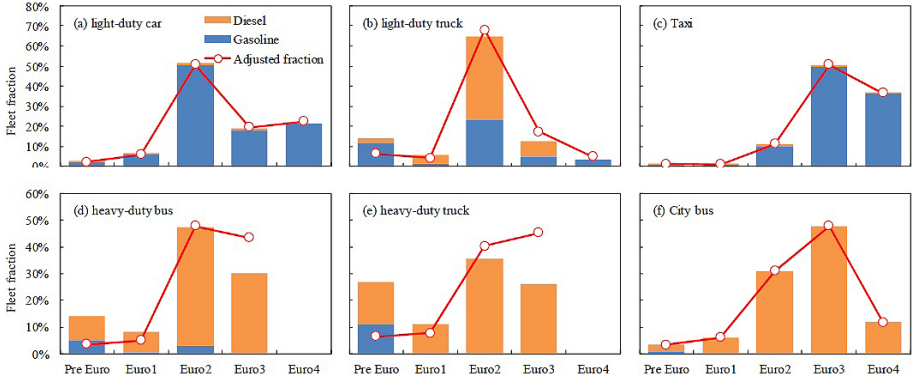

Figure 1. Static and adjusted fraction of the vehicle fleet in Shanghai, China.

ACPD
15, 7977–8015, 2015

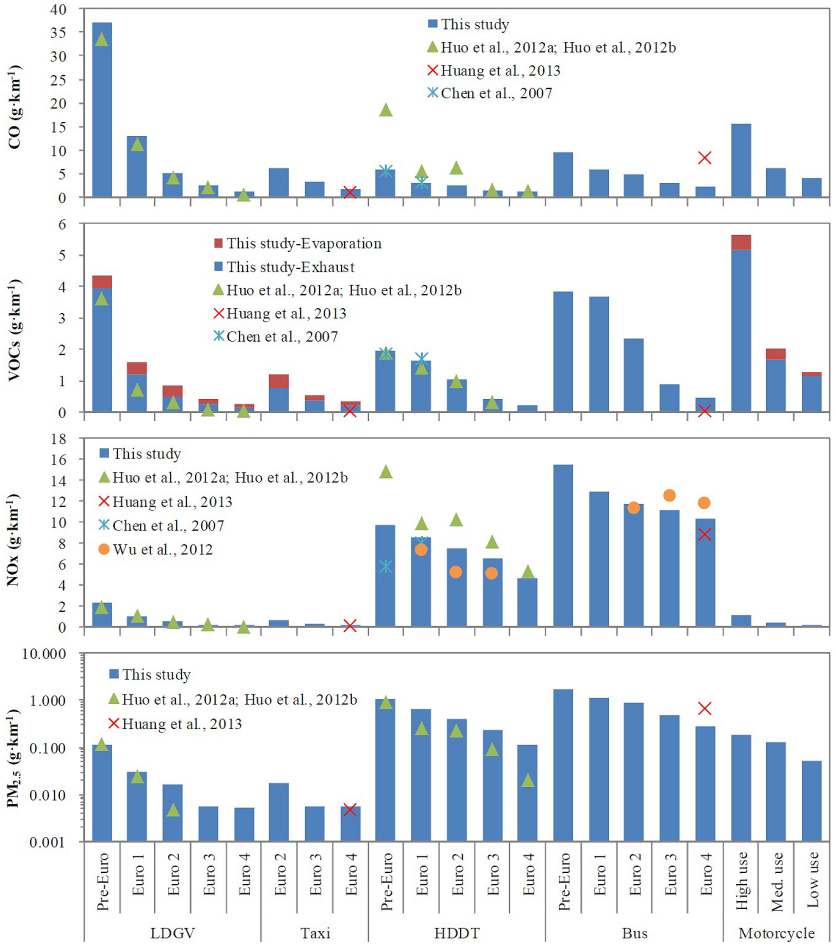

Figure 2. Calculated emission factors of various vehicle types and their comparisons with measured data.

ACPD
15, 7977–8015, 2015

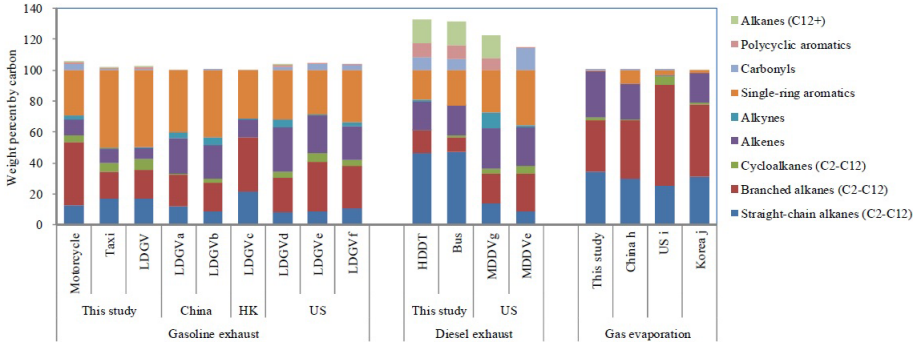

Figure 3. Comparisons of measured VOC compositions of the exhausts from different vehicle types and gas evaporation to the results in other studies (**a**: Liu et al., 2008; **b**: Wang et al., 2013; **c**: Guo et al., 2011; **d**: Schauer et al., 2002; **e**: May et al., 2014; **f**: Gentner et al., 2013; **g**: Schauer et al., 1999; **h**: Zhang et al., 2013; **i**: Harley et al., 2000; **j**: Na et al., 2004).

ACPD
15, 7977–8015, 2015

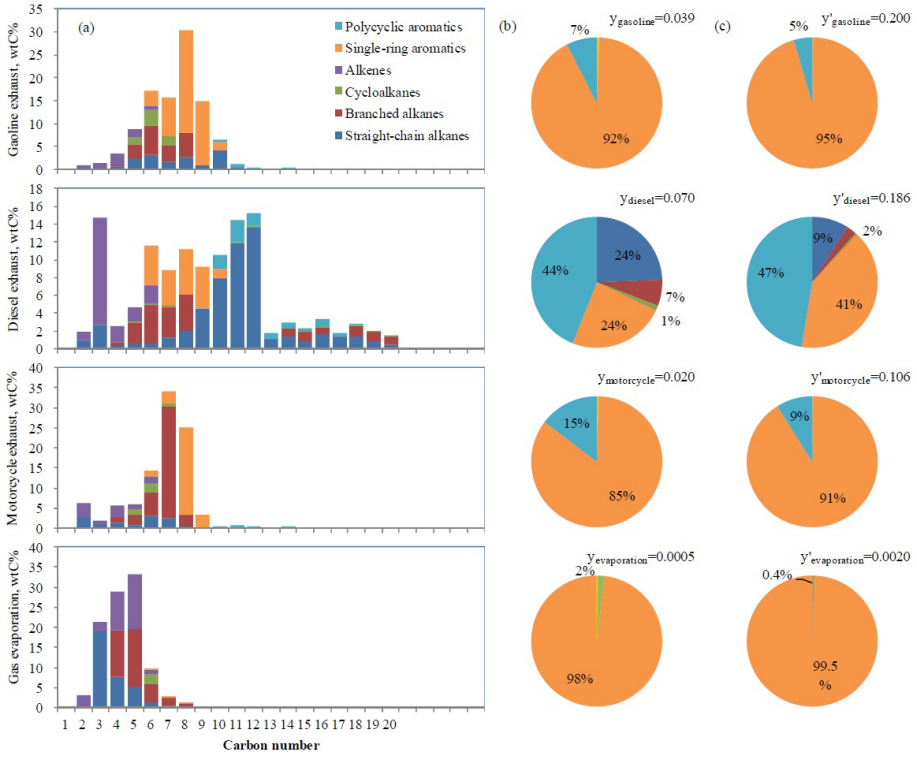

Figure 4. (a) Distribution of mass by chemical class in carbon number of different vehicle types and gas evaporation; **(b)** calculated SOA yields and their contributors of different vehicle types and gas evaporation; **(c)** calculated SOA yields under low-NO_x conditions.

ACPD
15, 7977–8015, 2015

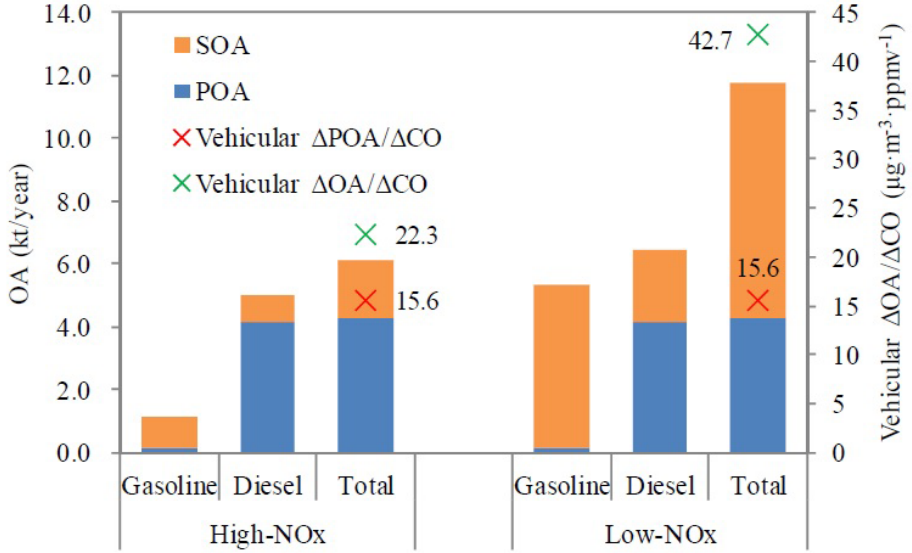

Figure 5. POA emissions from gasoline and diesel vehicles and their SOA formation potentials under high-NO_x and low-NO_x conditions.

ACPD
15, 7977–8015, 2015

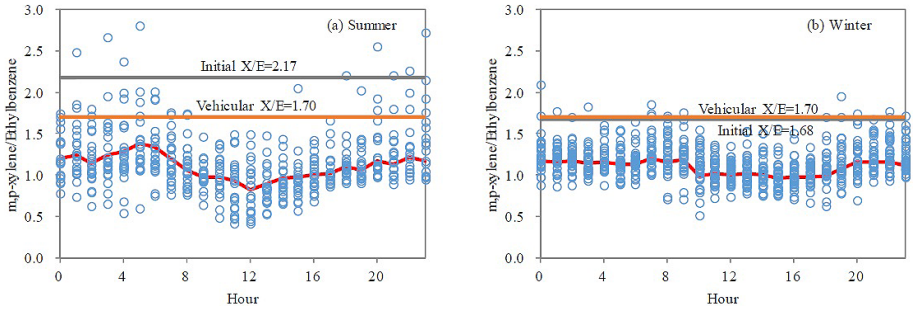

Figure 6. Diurnal distributions of the ratios of m, p-xylene to ethylbenzene concentrations in summer and winter in the urban atmosphere in 2013.

ACPD
15, 7977–8015, 2015

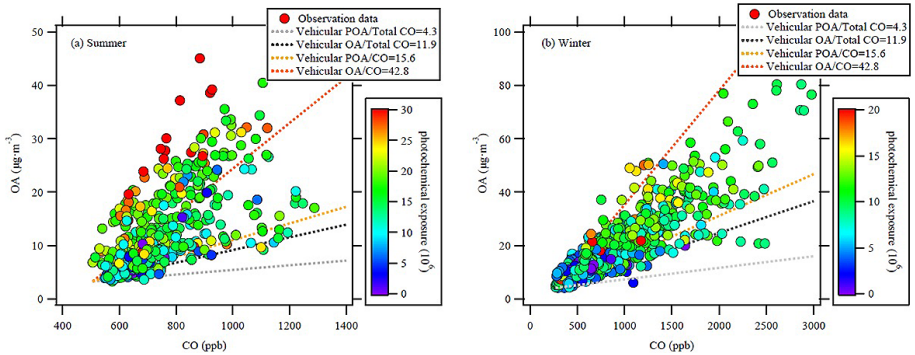

Figure 7. Relationship of measured OA and CO concentrations color-coded by the photochemical exposure in the summer **(a)** and winter **(b)** of 2013 in urban Shanghai according to Eq. (1). Vehicular POA/Total OA and Vehicular OA/Total OA were the ratios of vehicular POA emission and OA formation to total CO emission, respectively. Vehicular POA/CO and Vehicular OA/CO only considered vehicular CO emission. The SOA formations were calculated under low-NO_x conditions.

ACPD
15, 7977–8015, 2015

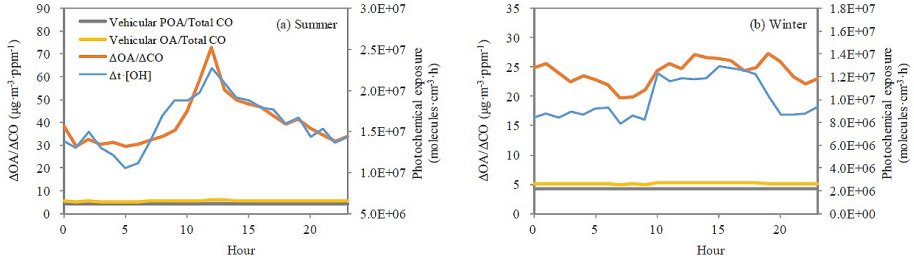

Figure 8. Diurnal variations of measured ΔOA/ΔCO in the atmosphere (red line), photochemical age Δ*t* (blue line) calculated by Eq. (1), and the ratios of vehicular POA (grey line) and vehicular OA (orange line) to total CO calculated by Eq. (2) in the summer and the winter of Shanghai, 2013.

ACPD
15, 7977–8015, 2015

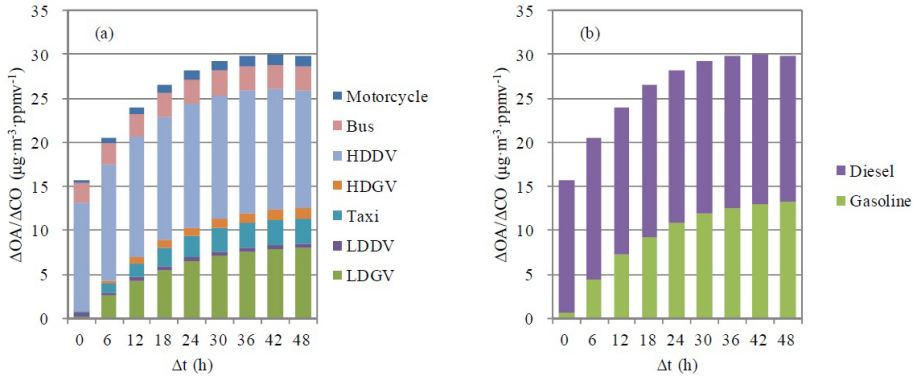

Figure 9. Contributions of vehicle emissions in different vehicle types **(a)** and fuel types **(b)** to OA formation ratios with the changes of photochemical ages.

ACPD
15, 7977–8015, 2015